



**HAL**  
open science

# Olivine composition and reflectance spectroscopy relationship revisited from advanced mgm deconvolution based on synthetic samples.

P.C. Pinet, Yves Daydou, Serge Chevrel

## ► To cite this version:

P.C. Pinet, Yves Daydou, Serge Chevrel. Olivine composition and reflectance spectroscopy relationship revisited from advanced mgm deconvolution based on synthetic samples.. Lunar Planetary Science Conference 52nd, Mar 2021, Houston, TX, United States. pp.#1422. hal-03441708

**HAL Id: hal-03441708**

**<https://hal.science/hal-03441708>**

Submitted on 22 Nov 2021

**HAL** is a multi-disciplinary open access archive for the deposit and dissemination of scientific research documents, whether they are published or not. The documents may come from teaching and research institutions in France or abroad, or from public or private research centers.

L'archive ouverte pluridisciplinaire **HAL**, est destinée au dépôt et à la diffusion de documents scientifiques de niveau recherche, publiés ou non, émanant des établissements d'enseignement et de recherche français ou étrangers, des laboratoires publics ou privés.

**OLIVINE COMPOSITION AND REFLECTANCE SPECTROSCOPY RELATIONSHIP REVISITED FROM ADVANCED MGM DECONVOLUTION BASED ON SYNTHETIC SAMPLES.** P.C. Pinet<sup>1,2</sup>, Y.H. Daydou<sup>1,2</sup> and S.D. Chevrel<sup>1,2</sup>. <sup>1</sup>Université de Toulouse; UPS-OMP; IRAP; Toulouse, France, <sup>2</sup>CNRS/CNES; IRAP; 14, avenue Edouard Belin, F-31400 Toulouse, France (patrick.pinet@irap.omp.eu).

**Introduction:** We revisit the behavior of the three primary olivine absorptions near 1  $\mu\text{m}$  (referred to as M1-1, M2, M1-2) and their interrelationships by means of an advanced version of MGM analysis. We build on the previous works carried out [e.g., 1, 2] to document at best the compositional variation of olivine from diagnostic absorption features across the visible and near-infrared wavelengths due to electronic transitions of Fe<sup>2+</sup> in the crystal structure.

**MGM implementation:** The principle of the Modified Gaussian Model is to deconvolve overlapping absorptions of mafic mineral spectra into their fundamental absorption components. Its specific interest is to directly account for electronic transition processes [e.g., 3]. The MGM approach is in essence able to achieve a direct detection and quantification of minerals. It is achieved by considering a sum of modified Gaussian functions characterized by their band centers, widths, and intensities. In the following, at the difference of a number of previous studies, the continuum is handled with a second-order polynomial initially adjusted on the local maxima along the reflectance spectrum (curvature, slope, and shift are free to move during the modeling) [4, 5, 6]. This is achieved by means of three anchor points searched within three spectral windows respectively spanning the intervals: 550-850, 1200-2000, 2300-2600nm. The robustness of modeling is also significantly increased with a set of starting conditions able to address situations ranging from laboratory to orbital data [4, 5, 6].

For the olivine MGM modeling, a set of 5 dedicated Gaussians (band center, band width, intensity and associated uncertainties) is used. The first Gaussian, centered around 450 nm, is used to model the strong large absorption at shorter wavelength (i.e. charge transfer in ultraviolet). The '650nm' Gaussian, though generally shallow, appears to handle absorptions possibly caused by transitions of minor elements such as Cr, Ni or other charge transfers.

Gaussian	Center (nm)	Width (nm)	Intensity
"450"	450±300	500±1000	-0.25±0.5
"650"	650±150	150±300	-0.25±0.5
M1-1	850±200	250±500	-0.25±0.5
M2	1050±200	200±500	-0.25±0.5
M1-2	1250±200	450±500	-0.25±0.5

**Olivine synthetic samples and spectral processing :** MGM inverse modeling provides with band center, band width and band depth estimates. Band centers are used to determine trend line equations for each individual absorption band M1-1, M2, M1-2, with an assessment on the regression performance (*rms* spectral distance between band center estimate from MGM and the one from the trend line). The olivine composition (Molar Forsterite *Fo#*) is then predicted based on minimizing the deviations in band centers from the established trends for the three absorptions simultaneously, using the integrated *rms* spectral distance to trend quantity (*sdt*).

Two suites of synthetic olivine samples, with small grain size (<45micron), are available and span the full range of stoichiometric olivine composition along the forsterite-fayalite solid solution series. The first suite is referred to as 'SUNY' (for State University of New York) and comprises 15 samples. The second suite includes 10 samples, prepared at Bristol University and referred to as 'BRISTOL' olivines.

A logical step is to implement our MGM deconvolution on each synthetic suite. The results of the MGM modeling outputs are displayed below for both suites. While for the band widths and strengths (Fig. 1.b), no obvious differences are noticed between the two suites, two trends are clearly found for the band centers (Fig. 1a), with a band center scattering significantly more pronounced for the Bristol suite (see below). For both suites, the scattering associated with the 850nm band center prevails over the 1050 and 1250 band centers ones (see Fig. 1a). Some samples markedly depart, in both suites, from the overall trends and call for caution. We also note that some Bristol samples tend to agree with the Suny trend.

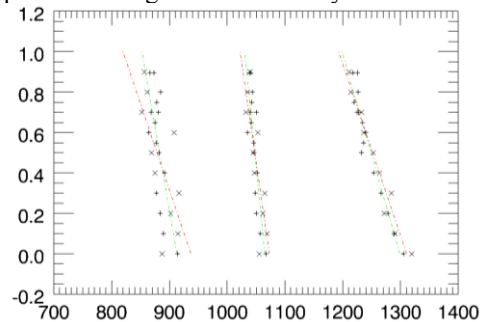


**Fig. 1.a** Band centers from MGM deconvolution for both suites (Symbol x is for "bristol" samples; symbol + is for "sunny"ones). Respective regression trend lines are displayed in green (Sunny) and red (Bristol).

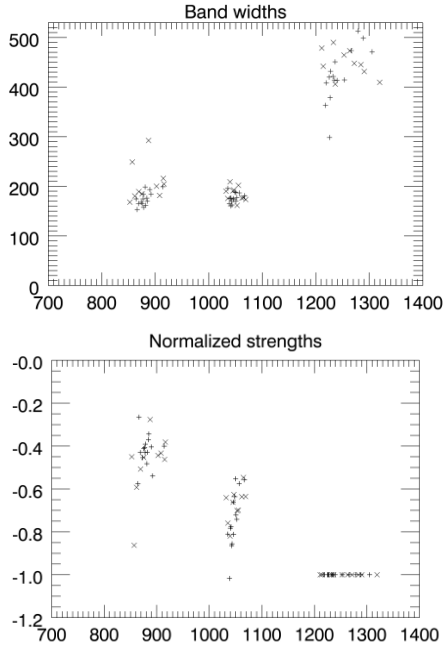


**Fig. 1.b.** Band widths and normalized strengths. (Symbol x is for "bristol" samples; symbol + is for "sunny"ones)

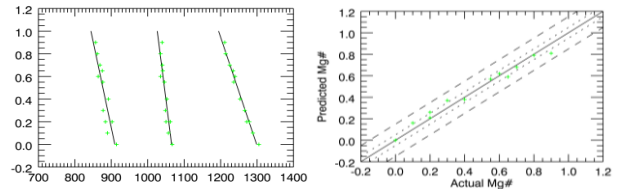
Quadratic distances (*rms*) to trend '850', '1050', '1250' and integrated spectral distance to trend *sdt* are given hereafter in nm. One obtains 24.4, 8.3, 7.4, **15.5** nm for the Bristol suite, and 11.5, 5.4, 7.5, **8.5** nm for the Sunny suite, respectively. This confirms the larger scattering of the '850nm' band associated with the M1-I absorption.

Based on these results, and on previous experimental analyses [7], it appears that the Sunny suite should be taken as the master list, and possibly completed by Bristol samples to reinforce the robustness of the trend line variations as a function of composition. However, as shown above, in both suites some samples depart from the overall trend. Accordingly, a series of tests is performed on various subsets selected from both Sunny and Bristol suites. For each subset of samples, a systematic testing of the coherency is performed to assess the performance of the regression, on the basis of the quantity *sdt* (more precisely, *rsdt*: real spectral quadratic distance to trend, associated with *Fo#*; *psdt*: predicted spectral quadratic distance to trend, associated with *Fô#*) and on the standard deviation (*rms*) associated with the *Fo#* estimates. The suite composed of 12 samples (9 Sunny, 3 Bristol) (see table1), which entirely spans the olivine composition domain from *Fo#*0 to *Fo#*90, is found to have the best consistency, in terms of *rsdt*, *psdt* and *Fo#* estimates (*rsdt*: 6.01nm, *psdt*: 4.94nm, *rms* "*Fo#-Fô#*":**0.046**). The regression so defined ( Fig. 2) is significantly more robust than either the Bristol (*rsdt*:15.5nm, *psdt*:10.9nm, *rms* "*Fo#-Fô#*":**0.110**) or Sunny (*rsdt*:8.5nm, *psdt*:5.8nm, *rms* "*Fo#-Fô#*":**0.087**) one considered separately.

This way we assess and mitigate, through the statistical consistency of the considered subset, the impact of the 'poor' quality of any given sample/spectrum [2,7] in the regression set to define the trend lines equations.

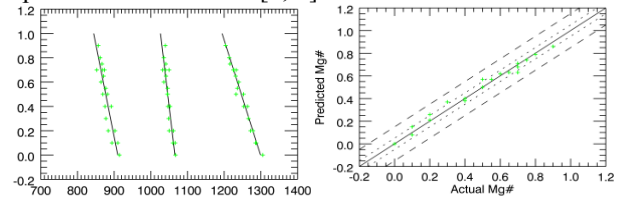
Name	MGM Conf.	Fo#	Fô#	Fo# - Fô#	real distance				predicted distance				
					<i>d</i> <sub>850</sub>	<i>d</i> <sub>1050</sub>	<i>d</i> <sub>1250</sub>	<i>rsdt</i>	<i>d</i> <sub>850</sub>	<i>d</i> <sub>1050</sub>	<i>d</i> <sub>1250</sub>	<i>psdt</i>	
DD-MDD-37	L5	0.90	0.81	-0.090	6.24	9.38	6.25	7.44	0.33	5.84	-3.17	3.84	
DD-MDD-38	L5	0.80	0.79	-0.010	4.44	1.21	-1.57	2.81	3.78	0.82	-2.62	2.70	
DD-MDD-116	L5	0.70	0.68	-0.020	4.88	1.97	-0.89	3.08	3.57	1.18	-2.98	2.77	
DD-MDD-90	L5	0.65	0.59	-0.060	8.21	1.44	3.37	5.19	4.26	-0.91	-2.91	3.03	
DD-MDD-91	L5	0.60	0.62	0.020	-6.35	-6.64	3.45	5.67	-5.04	-5.85	5.54	5.49	
DD-MDD-92	L5	0.55	0.57	0.020	3.14	1.97	-5.59	3.87	4.45	2.75	-3.50	3.63	
DD-MDD-94	L5	0.40	0.38	-0.020	8.45	2.64	-3.83	5.57	7.14	1.86	-5.92	5.46	
DD-MDD-95	L5	0.30	0.37	0.070	-12.61	-5.21	-1.46	7.92	-8.00	-2.46	5.86	5.90	
DD-MDD-96	L5	0.20	0.26	0.060	-12.65	-7.70	0.56	8.55	-8.70	-5.34	6.84	7.10	
DD-MDD-44	L5	0.20	0.21	0.010	5.63	4.13	-6.32	5.44	6.29	4.53	-5.27	5.41	
DD-MDD-97	L5	0.10	0.16	0.060	-13.78	-4.83	0.05	8.43	-9.84	-2.47	6.33	6.90	
DD-MDD-98	L5	0.00	0.00	0.000	4.40	1.63	5.97	4.39	4.40	1.63	5.97	4.39	
<i>RMS</i>					0.046	8.32	4.83	3.97	6.01	6.03	3.49	4.97	4.94

Table 1 Results for the considered 12 Suny-Bristol samples suite.



**Fig. 2.** Regression built from 12 samples suite (see table1).

The modeling can be improved for a few spectra by the addition of a couple of bands (2000, 2500nm) to handle minor contaminations. The same regression gives then very consistent results (Fig. 3) for 19 Suny-Bristol spectra (*rsdt*:6.12nm, *psdt*:5.49nm, *rms* "*Fo#-Fô#*":**0.036**), the 6 ones discarded being subject to impurities, concerns in the sample preparation or the spectral measurements [2, 7].



**Fig. 3.** Results with 19 samples Suny-bristol suite.

**Conclusions:** The trend lines equations derived from the current MGM modeling are more robust than previous solutions [1, 2, 8]. The band center positions of the three primary olivine absorptions (M1-1, M2, M1-2) are used simultaneously to produce a constrained prediction across an extended range *Fo#*[0-90] of olivine composition with synthetic or natural samples.

**References:** [1] Sunshine J. M. and C. M. Pieters (1998) *JGR*, 103, 13,675–13,688. [2] Isaacson P.J. et al (2014) *Am. Miner.*, 99, 467-478. [3] Sunshine J.M. et al. (1990) *JGR*, 95, B5, 6955-6966. [4] Clenet, H. et al. (2011) *Icarus*, 213, 404-422. [5] Clenet, H. et al. (2013) *JGR*, 118, doi:10.1002/Jgre.20112. [6] Pinet P.C. et al. (2019) *LPSC L*, Abstract #1806. [7] Dyar M.D. et al. (2009) *Am. Miner.*, 94, 883-898. [8] Han, H-J. et al, (2020) *Res. Astr. Astroph.*, 20, 129.